THE TOPOGRAPHIC CHARACTER OF THE LARGEST CANDIDATE IMPACT CRATERS ON BENNU.

R.T. Daly[1], E.B. Bierhaus[2], O.S. Barnouin[1], M.G. Daly[3], J. Seabrook[3], J.H. Roberts[1], C.M. Ernst[1], M.E. Perry[1], E.E. Palmer[4], R.W. Gaskell[4], J.R. Weirich[4], H.C.M. Susorney[5], C.L. Johnson[4,5], K.J. Walsh[6], M.C. Nolan[7], E.R. Jawin[8], P. Michel[9], D. Trang[10], and D.S. Lauretta[7]. [1]Johns Hopkins Applied Physics Laboratory, Laurel, MD (terik.daly@jhuapl.edu); [2]Lockheed Martin Space, Littleton, CO; [3]Centre for Research in Earth and Space Science, York Univ., Toronto, Ontario, Canada; [4]Planetary Science Institute, Tucson, AZ; [5]Dept. of Earth, Ocean & Atmospheric Sciences, Univ. of British Columbia, Vancouver, Canada; [6]Southwest Research Institute, Boulder, CO; [7]Lunar and Planetary Laboratory, Univ. of Arizona, Tucson, AZ; [8]Smithsonian National Museum of Natural History, Washington, D.C.; [9]Université Côte d'Azur, Observatoire de la Côte d'Azur, CNRS, Laboratoire Lagrange, Nice, France; [10]University of Hawa'ii, Honolulu, HI.

Introduction: Data from the OSIRIS-REx mission revealed that (101955) Bennu has hundreds of candidate impact craters [1], henceforth called "impact craters" for ease. Impact craters provide clues to the physical properties of Bennu's surface and interior. Cratering on Bennu occurs in a challenging regime: gravity is very weak [2,3]; target strength is quite low [2,3], but poorly known, and could vary with depth; target porosity is high [3,4]; and the target surface is very coarse-grained and boulder-rich [2,5]. Here we report the latest assessment of impact crater depth-to-diameter ratios, *d/D*, on Bennu, with a focus on results from the OSIRIS-REx Laser Altimeter (OLA) and the clues that large craters provide about Bennu's interior structure.

Methods: OLA collected over 3 billion altimetric returns during a ~six-week span in summer 2019 [6]. Co-registered OLA scans were used to make regional digital terrain models (DTMs) of all impact crater candidates >10 m in diameter (135 total). The DTMs have a ground-sample distance (GSD) of 10 cm. Some craters were excluded from the analysis for reasons such as overlap with another depression. From each regional DTM, we extracted topographic profiles across each crater at eight different azimuths. Rim-to-rim diameter and rim-to-floor depth were determined along each profile. Profiles were excluded if they passed through an irregularity (e.g. large boulder) on the rim. The remaining profiles were averaged to compute the rim-to-rim diameter, rim-to-floor depth, and *d/D* for each crater.

The results shown here were measured with respect to elevation, with a correction applied to account for regional slopes. Earlier reports [7,8] did not apply this correction, which accounts for differences in the values reported here vs. the values in [7,8]. The slope correction does not change the trends in *d/D* reported previously.

To aid analysis of the larger craters, a global shape model of Bennu was decomposed into spherical harmonics [4,9]. Long-wavelength reconstructions of the shape were then generated by including only the spherical harmonic components out to a degree and order corresponding to a wavelength of interest.

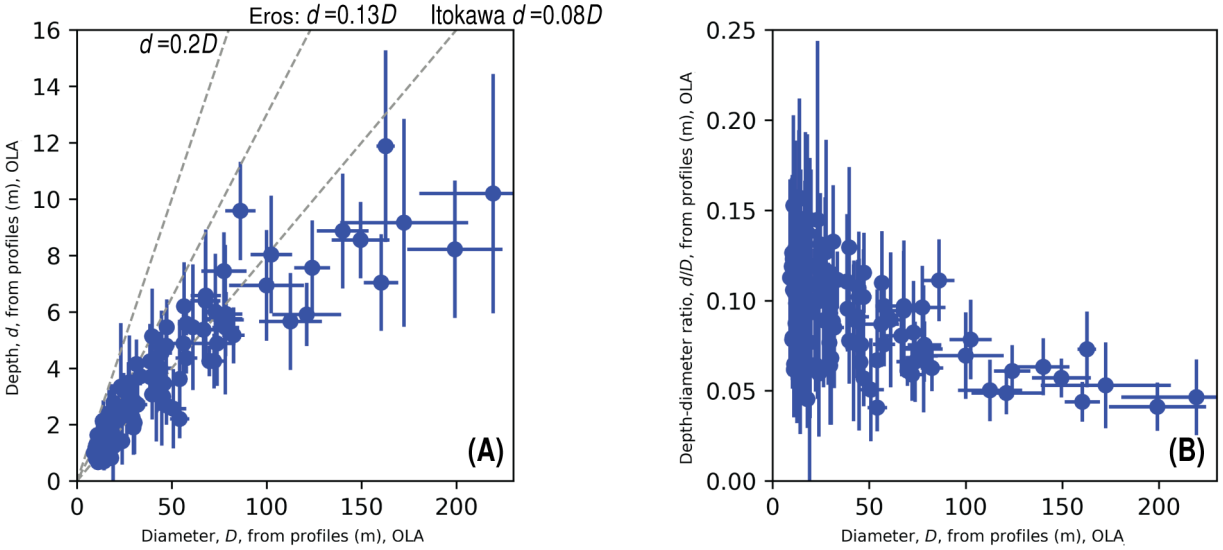

Figure 1. (A) The diameters and depths of craters larger than 10 m on Bennu. As points of reference, dashed lines in (A) indicate the *d/D* ratios for typical terrestrial planets (d=0.2D), the asteroid Eros [10], and rubble-pile asteroid Itokawa [11]. (B) Plotting *d/D* as a function of crater diameter emphasizes the tendency for large craters to be shallow.

Results: Impact craters on Bennu have a wide range of *d/D* (Fig. 1). With respect to elevation, *d/D* varies from 0.04 to 0.16. Craters exhibit a range of depths, with the largest variation at smaller crater sizes. The larger craters (~>100 m) are all shallow.

Discussion & Implications: Prior work [7,8] addressed possible reasons for the broad range of *d/D* ratios of impact craters on Bennu. Here we focus on the fifteen largest impact craters (>100 m diameter). Post-impact modification (e.g., infill) could also contribute to small *d/D* ratios. These large craters are presumably some of the oldest on Bennu, which gives mass wasting/infilling processes a long time to operate. However, not all large craters show evidence for mass wasting. A gravitationally driven collapse process (such as the one that leads to shallow, complex craters on larger bodies) is not viable in the microgravity environment of Bennu. A more competent layer at depth can lead to crater flattening as seen on the Moon, thereby decreasing *d/D* [e.g., 12]. Bennu's shape and topography implies a stiffness [4] that could be consistent with increased strength at depth.

Target curvature may also be an important factor. The average radius of Bennu is 245 m [4]; hence, craters >100 m subtend a solid angle that represents a significant fraction of the body (Fig. 2).

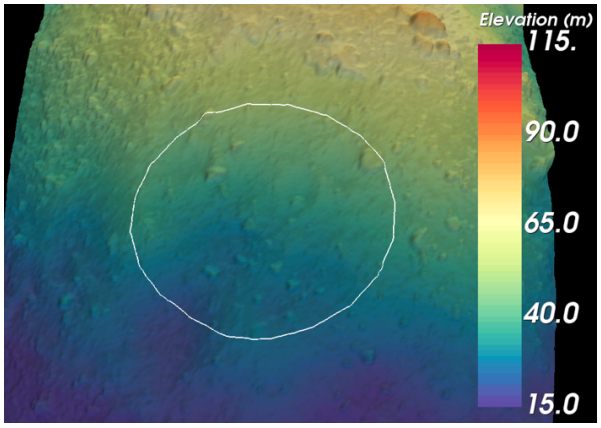

Figure 2. 10-cm GSD OLA DTM of a ~150-m-diameter crater candidate centered at 55.73° N 62.70° E. The DTM is colored by elevation; the white ellipse marks the approximate crater rim. This single crater covers ~2% of Bennu's surface area. It is located on a regional slope. Its *d/D* is 0.06 with respect to elevation.

These large, shallow craters are often flat and facet-like with respect to geometric height. It is as though something sliced off part of the global shape of Bennu, leaving behind, in some cases, only the subtlest rims. Figure 3 compares the global shape model of Bennu (cream color) to a low-degree (degree 12) spherical harmonic reconstruction of the global shape model (yellow). The wavelength of the degree-12 model is ~130 m, comparable to the length scale of the crater.

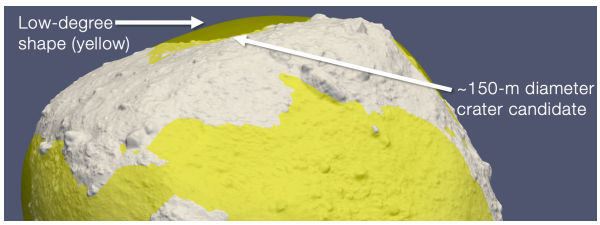

Figure 3. Comparison between a high-res. global shape model of Bennu (cream color) and a degree 12 spherical harmonic reconstruction of the global shape. This figure views the crater in Fig. 2 roughly edge-on. In this view, the crater in Fig. 2 is located at about the 11 o'clock position on the limb of the high-resolution global model.

Impact experiments reported by [13] into curved mortar cylinders or semi-spheres yielded a range of crater morphologies similar to those observed in the large craters on Bennu, including cases where the impact resulted in a very shallow crater with a muted rim and the impact created a flat facet with no rim. The impacts in [14] were into strength-controlled targets, not a rubble pile. However, Bennu's global topography implies stiffness [4] and the center-of-mass/center-of-figure offset could be explained by a few large boulders or shards in the interior of Bennu [3]. The unusual morphologies of the largest craters on Bennu may be an additional line of evidence that, at large scales, Bennu possesses strength, despite being a rubble pile.

Acknowledgements: This material is based on work supported by NASA under contract NNM10AA11C issued through the New Frontiers Program. We are grateful to the entire OSIRIS-REx team for making the Bennu encounter possible. This work used the Small Body Mapping Tool (sbmt.jhuapl.edu). P.M. acknowledges support from the French space agency, CNES.

References: [1] Bierhaus E.B. et al. (2019) *LPSC L,* abs. 2469. [2] Lauretta D.S. et al. (2019) *Nature*, 568, 55–60. [3] Scheeres D.J. et al. (2019) *Nat. Astron.* 3, 352–361. [4] Barnouin O.S. et al. (2019) *Nat. Geosci.,* 12, 247–252. [5] Walsh K.J. et al. (2019) *Nat. Geosci.,* 12, 242 – 246. [6] Daly M.G. (2017) *Space Sci. Rev.,* 212, 899–924. [7] Daly R.T. et al. (2019) *LPSC L,* 1647. [8] Daly R.T. et al. (2019) *Asteroid Science in the Age of Hayabusa2 and OSIRIS-REx,* 2030. [9] Roberts J. et al. (2020), *LPSC 51,* this meeting. [10] Barnouin-Jha O.S. et al. (2001) *LPSC XXXII,* abs. 1786. [11] Hirata N. et al. (2009) *Icarus,* 200, 486–502. [12] Quaide W.L. and Oberbeck V.R. (1968) *JGR,* 73, 5247–5270. [13] Fujiwara A. et al. (1993) *Icarus*, 105, 345–350.